ACS OMEGA

Open Access

http://pubs.acs.org/journal/acsodf

Article

What is the Diatomic Molecule with the Largest Dipole Moment?

Ahmed Elhalawani, Ruiren Shi, Mateo Londoño, Michał Tomza, and Jesús Pérez-Ríos*

Cite This: *ACS Omega* 2026, 11, 17286−17291

Read Online

ACCESS | Metrics & More | Article Recommendations | Supporting Information

ABSTRACT: We present a machine learning model to predict the electric dipole moment of diatomic molecules using only the atomic properties of the constituent atoms. The model can screen the entire periodic table to identify the molecules with the largest dipole moments for applications in cold molecular sciences or to find the molecule with the largest dipole moment that contains a given atom. Similarly, our model identifies useful trends that explain molecular dipole moments, improving our intuition in chemical physics beyond the paradigm of electronegativity differences. Finally, we condense our model into an analytical expression to predict the dipole moment in terms of atomic properties.

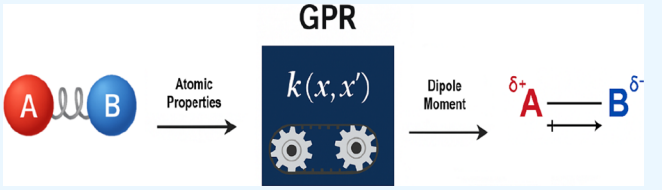

INTRODUCTION

The electric dipole moment is an intrinsic property or fingerprint of molecules; hence, every molecule has a different one. The dipole moment of a chemical plays a significant role in its physicochemical properties, such as melting point,[1] solubility,[2] and thermal conduction,[3] to cite a few. In cold molecular sciences, the search for diatomic molecules with large dipole moments is one of the most active research areas due to its prospective applications in dipolar quantum gases, the development of quantum gates based on polar molecules,[4−9] implementation of new Hamiltonians and the study of many-body physics,[10−15] among others. Similarly, the search for new physics with molecules can benefit from molecules with larger dipole moments, especially those containing radioactive atoms like Fr−Y for hadronic charge-parity violation searches[16,17] and Ra−Y for measuring the electric dipole moment of the electron as a consequence of charge-parity-time-reversal symmetry violation.[18,19]

The dipole moment of molecules is either experimentally determined by spectroscopic techniques or calculated using ab initio quantum-chemical methods.[20,21] However, neither of these routes is a plausible approach for determining the dipole moment of the possible 6903 polar diatomic molecules. In principle, one can resort to the chemical intuition to find molecules with the largest difference in the electronegativity within the atoms and, with it, the largest dipole moments due to a larger ionic character.[22−25] However, it has recently been found that X−Ag molecules, where X is an alkali-metal atom, exhibit large dipole moments, which is unexpected given the predicted minor ionic character these molecules should exhibit, since the two atoms have similar electronegativities.[16,26] Based on these results, it is certainly not a trivial task to find out which diatomic molecules can show a large dipole moment.

In this paper, we employ a machine learning approach to predict the dipole moment of diatomic molecules based on atomic properties. As a result, it is possible to screen the whole set of polar diatomic molecules and find which molecules have the largest dipole moment, or to find the molecule containing a given atom type that shows the largest dipole moment. In the same vein, our machine learning models help us identify unforeseen patterns in the dipole moments of molecules based on groups and periods, which are tested against high-level ab initio electronic structure methods and confirmed. Therefore, a machine can teach us more about the nature of the dipole moment and its interconnection with essential atomic properties than anticipated. In line with these findings, we use symbolic regression to identify a simple, data-driven relationship that predicts the dipole moment with an accuracy of better than one Debye.

METHODOLOGY

As introduced by Pauling,[22] the polarity of a bond is a direct consequence of atoms having different specificities to attract electrons, known as electronegativity χ. Therefore, it is possible to describe the partial ionic character in terms of the electronegativity, and surprisingly enough, there is no unique way to do so. Pauling proposed

$$\mathrm{IC_P} = 100(1 - \mathrm{e}^{-|\chi_1-\chi_2|^2/4}) \tag{1}$$

where χ_i is the electronegativity of the i-th atom in the molecule. Alternatively, Hannay and Smyth[24] proposed

$$\mathrm{IC_{HS}} = 16|\chi_1 - \chi_2| + 3.5|\chi_1 - \chi_2|^2 \tag{2}$$

Received: September 18, 2025
Revised: January 25, 2026
Accepted: January 28, 2026
Published: March 9, 2026

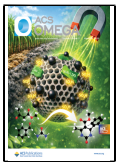

Both of these definitions, eqs 1 and 2 lead to very different partial ionic characters, even thought both of them were empirically derived.[1]

Additionally, as shown beautifully in the seminal work of Coulson,[27] the dipole moment has contributions beyond bond polarity, such as the homopolar dipole moment, which depends on the size of the atom, or the anisotropy of the atomic orbitals. Therefore, the relationship between the dipole moment and the partial ionic character may not be as straightforward as thought and may depend on properties beyond electronegativity. However, the idea that the electronegativity difference between atoms within a molecule yields a large ionic character and, with it, a large dipole moment has spread in modern chemistry, and even advanced large language models fail to predict the dipole moment of molecules.

The dipole moment, as it is taught in elementary chemistry courses, is defined as

$$d = qR_e \tag{3}$$

where q is the effective separated charge and R_e denotes the equilibrium bond length of the molecule. As introduced by Pauling, the dipole moment is related to the polarity of molecular bonds, describing the partial ionic character of the bond, given by

$$\mathrm{IC_d} = 100\frac{d}{eR_e} \tag{4}$$

where e is the electron charge, and the result is given in %.

Here, we pursue a machine learning approach. To learn the dipole moment of diatomic molecules, we compile a data set comprising 273 molecules. Of these, 140 have experimentally measured dipole moments.[28−44] At the same time, the remaining 133 have theoretically calculated dipole moments[26,45−47] using the gold standard in quantum chemistry: Coupled clusters with singles, doubles and perturbative triple excitations [CCSD(T)], in conjunction with large enough correlation-consistent basis sets and, when needed, the inclusion of Stuttgart/Koeln fully relativistic multielectron fit effective core potential (ECPnMDF), to model the first n core electrons (see Supporting Information). This ab initio methodology is adequate for the determination of most of the diatomics.[48] First, we noticed that the relationship between the dipole moment and the equilibrium distances, using eq 3, yields a rather dispersed value of q, as shown in Figure 1A. Certainly, it deviates from the extreme case of $q = e$, except NaF and SrO (both highlighted in Figure 1A). Therefore, the relationship between the dipole moment and the equilibrium distance is not linear at all for some molecules. To explore the variety of bonding and chemical behavior within this set, we employ the van Arkel−Ketelaar Triangle,[49,50] as customary in inorganic chemistry to identify the nature of chemical compounds, as shown in Figure 1B. Molecules closer to the tip of the triangle are those with a larger ionic character (ionic bond), the ones in the right corner show a covalent bond, and the ones in the left corner are van der Waals molecules.[2] The data set shows a relatively uniform distribution across these three bonding types, with a slight skew toward van der Waals-type bonding. Interestingly, we noticed that some molecules far from the tip of the triangle exhibit a large dipole moment, even though their expected ionic character is not large, contradicting general chemical intuition and classification. In particular, the molecules CsI (11.69 D), RbBr (10.86 D), and

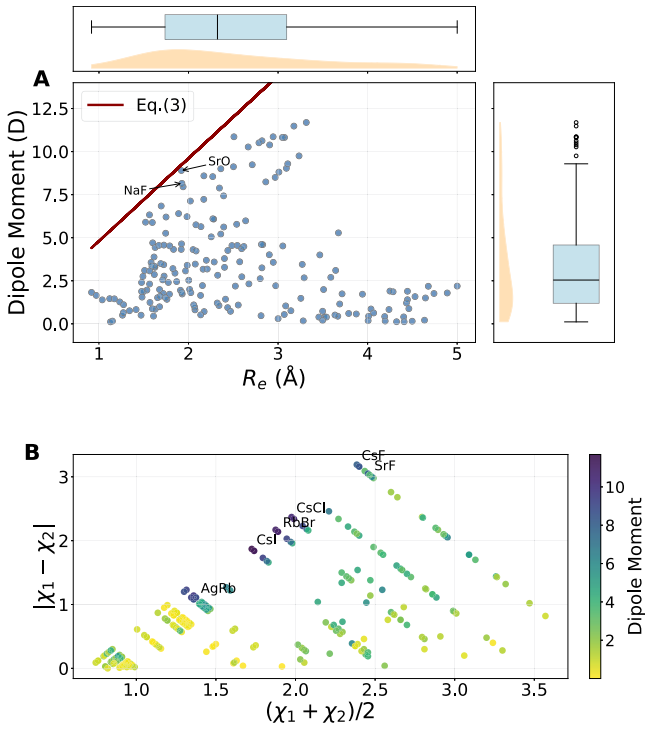

Figure 1. Dipole moment of diatomic molecules data set containing experimental and accurate theoretical data. (A) Dipole moment (in Debye) versus the equilibrium distance (in Angstrom), as well as the maximal predicted values from eq 3 (for $q = e$) as a line and the 2 molecules with values closest to this prediction. Additionally, it shows box plots for the dipole moment and equilibrium distance. The box plot shows the minimum, the maximum, the sample median, and the first and third quartiles of a given distribution. (B) Van Arkel−Ketelaar's triangle of the data set, as characteristic in inorganic chemistry to characterize metallic (left corner), ionic (top corner), or covalent compounds (right corner).

CsCl (10.387 D) have much larger dipole moments compared to the ionic bond molecules such as CsF (7.88 D), SrF (3.47 D). What is more remarkable is that there are molecules with a low difference in electronegativity that have comparable dipole moments to ionic bond molecules, such as AgRb (9.03 D) and AgCl (5.62 D).

We employed Gaussian Process Regression (GPR) as one of our primary predictive models because of its advantages in low-data settings.[51] GPR provides not only point predictions but also uncertainty estimates, which are valuable when applying the model to extrapolate. Additionally, we compare our GPR models against baseline models, including Support Vector Regression (SVR), random forest, and Gradient Boosting Regression (GBR), using a consistent validation scheme to ensure a fair comparison. To validate our models, we adopted a Monte Carlo Cross-Validation (MCCV) scheme,[52] modified to prevent data leakage from duplicated entries. In each iteration, we randomly split the data set into 90% training and 10% testing. This split was done based on the molecule's name (both the forward and backward versions have the same name in our data set), ensuring that both the original and swapped entries for any given molecule were confined to the same split. This approach prevents information about a molecule in the training set from benefiting predictions on the test set. For all these models, we utilize a modified ionic character provided by eq 2 $\sqrt{\mathrm{IC_{HS}}}$ and the difference in ionization potentials (IP)

https://doi.org/10.1021/acsomega.5c09766
ACS Omega 2026, 11, 17286−17291

$\Delta_{IP}^{1/4}$ where $\Delta_{IP} = |IP_A - IP_B|$ and also the reciprocal product of the ionization potentials $\frac{1}{IP_A IP_B}$ and the sum of the electron affinities (EA) $(EA_A + EA_B)$ for both atoms as numerical features. Additionally, we include the group and period of each atom in the molecule as categorical features. It is not surprising that the ionization potential and electron affinity appear as features, since they explain an atom's ability to attract electrons. In contrast, the latter explains its ability to donate electrons. Similarly, ionic character is expected in the feature vector, as it accounts for the charge mismatch in a molecule's chemical bond. What is surprising, at first sight, is the particular functional form in which those properties enter as a feature. However, these functional forms result from a more accurate representation of the data, thereby improving the efficiency of the machine learning algorithm.

RESULTS AND DISCUSSION

We ran 1000 iterations within the MCCV procedure and computed the average Root Mean Square Error (RMSE) and Mean Absolute Error (MAE) across all runs. The model's performance, as measured by the MAE and RMSE, is presented in Table 1. Therefore, the model depends only on atomic properties. GPR outperforms the other models, with an RMSE of 0.67 D, followed by Gradient Boosting Regression. Therefore, from now on, we will focus on the GPR model, and its results are shown in Figure 2. The model presents a few inaccurate predictions like BaS, MoC, and some van der Waals molecules like LiNa, NaCs, and LiCs, also inaccurate predictions even when molecular properties are included; possibly related to an anomalous natural bond orbital atomic charge versus the Mulliken charge for each of these molecules.[53]

Previous attempts to predict the dipole moment of molecules required molecular properties or structural information.[53−58] Although accurate, they are hardly extrapolable to unknown molecules, since their molecular properties are also unknown. On the contrary, we can bypass this problem by using only atomic properties. In that regard, guided by the model's accuracy, we search for the diatomic with the largest dipole moment. Since our model requires the ionic character and, with it, the electronegativities of the atoms, we screen 4851 molecules, as only 99 elements have reliable electronegativities within the Pauling scale. The results of our model are shown in Figure 3, where some unseen molecules predicted by the model are contrasted with CCSD(T) calculations. First,

Table 1. Comparison of Regression Methods Based on RMSE and MAE (in Debye)[a]

ML method	RMSE	MAE
GPR training set	0.10	0.07
Gaussian process regression	0.67	0.45
gradient boosting	1.00	0.70
random forest	1.05	0.70
support vector regression	1.07	0.77
PySR model	1.27	0.96

[a]The training set results refer to the Gaussian process regression model.

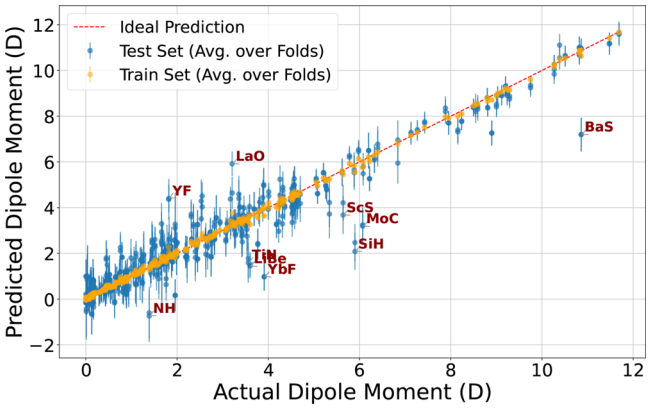

Figure 2. Prediction of the dipole moment of diatomics. Predicted dipole moment versus the real dipole moment. The error bars represent the associated uncertainty for each prediction, and the dashed red line represents the perfect prediction. The color scheme indicates whether a point belongs to the training set (orange) or the testing set (blue). The labeled points are inaccurate predictions with |Predicted − Actual| > 1.5 D.

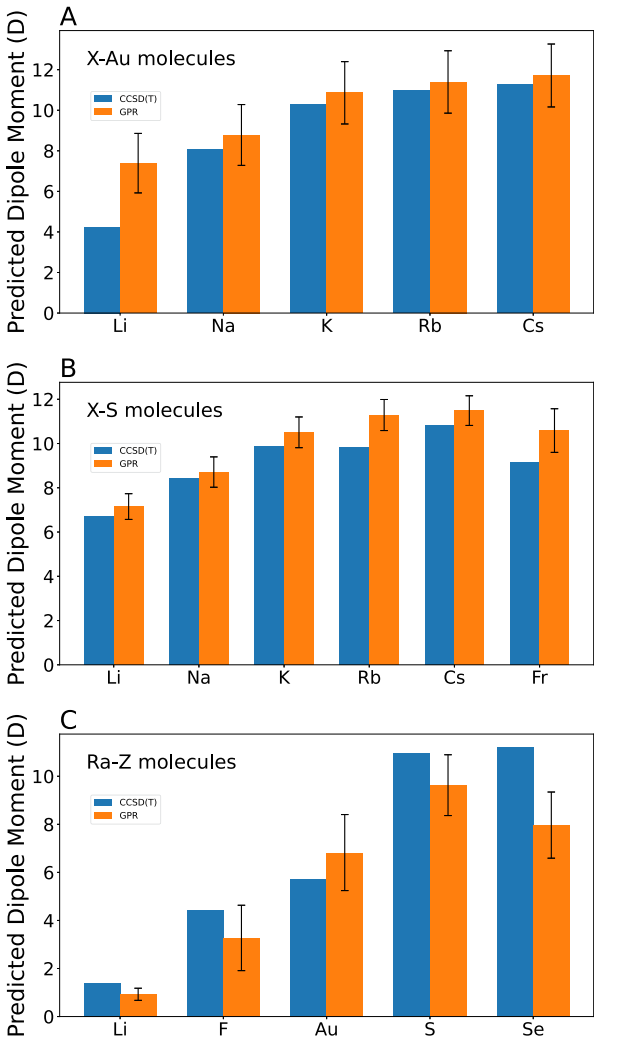

Figure 3. Testing the machine learning model predictions on 4851 molecules. (A and B) Predicted dipole moments for X−Au and X−S molecules (X = Alkali-metal) against CCSD(T), respectively. The machine learning model has never seen these molecules. (C) Theoretical dipole moment for radium-containing molecules (ordered by CCSD(T) smallest to largest) versus GPR predictions. Across all 3, the trends of CCSD(T) are captured in the GPR predictions.

https://doi.org/10.1021/acsomega.5c09766
ACS Omega 2026, 11, 17286−17291

we notice that the model is surprisingly accurate in predicting the dipole moment of unseen molecules in comparison with CCSD(T) calculations, even when some molecules are in the extrapolation regime, i.e., molecules unseen by the model, where machine learning techniques are supposed to lose accuracy. This confirms the robustness of our machine learning model. More importantly, the machine correctly captures the trend for X−Au and X−S molecules, where X is an alkali atom. In other words, the machine can reveal the underlying correlations between the dipole moment and the atomic properties of the atoms that form the molecule. A more detailed study on the properties of the model is provided in the Supporting Information.

Recently, it has been demonstrated that alkali-Ag molecules exhibit a significant dipole moment, despite the slight electronegativity difference between Ag and alkali atoms. This result is very puzzling. However, as we show in Figure 3A, alkali-Au molecules show the same trend. Indeed, the dipole moment of alkali-Au molecules is larger than that of alkali-Ag molecules—another example of molecules with a relatively small electronegativity difference showing a large dipole moment. Why is that? The reason is that the group 11 atoms are transition metals with a hole in the valence shell, so they can be seen as the *halogens* of the transition metals. As any halogen, the largest dipole is when those are in contact with alkali atoms (alkali halides), hence explaining why Cu-, Ag-, and alkali-Au have a large dipole moment. For alkali halides, the dipole moment grows as the period of the halogen atom. Thus, explaining why alkali-Au molecules show a larger dipole moment than alkali-Ag molecules. Following that trend, alkali-Rg may show even larger dipole moments from any of the group 11 elements combined with alkali atoms, although relativistic contributions may affect the dipole moment and end up comparable to alkali-I molecules. On the other hand, in Figure 3B, we notice that alkali metal monosulfide molecules show a pretty significant dipole moment, which should not come as a surprise since the alkali metal oxides show a decent dipole moment, keeping in mind that S is a period 3 atom, whereas O shows a period 2. Similarly, alkaline earth oxides exhibit a large dipole moment, perhaps related to the fact that the chalcogens can be viewed as p-shell atoms with two holes, each filled by the two valence electrons of the alkaline earth metals. Therefore, earth metal monosulfide compounds will also show a large dipole moment, genuinely larger than those of alkaline earth metal oxides.

Another possibility our model offers is to find the molecule with the largest dipole moment that contains a given atom. To test this capability, we predict the radium-containing molecules with the largest dipole moments, and the results are shown in Figure 3C against CCSD (T) calculations. Again, the GPR model is unexpectedly good at predicting the dipole moment, although RaSe seems somewhat difficult for the model. More importantly, thanks to this exploration, we can confirm that RaS or RaSe are promising candidates for the study of radium-containing molecules in the cold regime, and their laser cooling possibilities will be the subject of future work.

After the exhaustive screening, we identify the top 20 molecules with the largest dipole moment, and the results are shown in Table 2 in comparison with CCSD(T) calculations and experimental data, when available. The GPR results are pretty good compared to CCSD(T) calculations. The molecule with the largest dipole moment will be the combination of the heavy alkali halides X−I or X−At, followed by alkali-Au molecules, which can be viewed as the combination of the heaviest halogen transition-metal atom and alkali.

Table 2. Top 20 Molecules with High Dipole Moments: Ordered First by Descending CCSD(T) Values (When Available) and Then by Descending GPR Predictions[a]

molecule	experimental	CCSD(T)	GPR prediction	symbolic regression
CsI	11.69	11.73	11.52 ± 0.48	12.15
FrI	N/A	11.63	10.92 ± 0.85	11.89
RbI	11.48	11.41	11.16 ± 0.46	11.14
AuCs	N/A	11.25	11.82 ± 0.93	10.86
RaSe	N/A	11.20	7.98 ± 0.9	5.71
BaSe	N/A	11.18	8.59 ± 0.61	5.90
CsSe	N/A	11.0	10.58 ± 0.77	9.39
AuRb	N/A	10.97	11.76 ± 0.86	9.99
RbBr	10.86	N/A	10.97 ± 0.43	11.35
BaS	10.86	10.89	10.59 ± 0.19	5.73
RbSe	N/A	10.83	10.71 ± 0.74	8.65
CsS	N/A	10.82	11.49 ± 0.67	9.09
CsBr	10.82	N/A	10.96 ± 0.47	12.41
SrSe	N/A	10.65	6.21 ± 1.29	5.07
SrS	N/A	10.62	6.83 ± 1.37	4.94
AuK	N/A	10.30	11.10 ± 0.85	9.61
CaSe	N/A	10.03	6.71 ± 0.65	4.56
AuFr	N/A	9.93	11.53 ± 0.98	10.67
RbS	N/A	9.82	11.29 ± 0.70	8.37
CsCl	N/A	N/A	10.89 ± 0.48	12.39

[a]Experimental and symbolic regression values are shown for comparison.

To complement our machine learning models, we also applied symbolic regression via PySR[59] to find an analytical formula for the dipole moment of a molecule, AB, in terms of atomic properties

$$d = \left| \Delta_{\mathrm{IP}}^{1/4} + \left((\mathrm{EA_A} + \mathrm{EA_B}) \cdot \left(\sqrt{\mathrm{IC_{HS}}} \cdot \left(\frac{24.43}{\mathrm{IP_A IP_B}} - 0.14 \right) \right) \right) \right| \tag{5}$$

The symbolic model achieved an RMSE of 1.26 D on the original test data and, when used on the same set of 4851 theoretical molecules, produced an RMSE of 0.92 D, as shown in Table 1, capturing many of the same trends as the machine learning model with reduced precision. The predictions of this model for the top 20 molecules are displayed in Table 2, showing a good agreement with experimental and CCSD(T) results, for most of the molecules. The symbolic model offers interpretability and analytic insight that is not as visible when using GPR alone. In other words, we found the most reliable expression for the dipole moment of diatomics.

CONCLUSIONS

In summary, we have demonstrated that the general idea that the difference in electronegativity determines the polarity of the molecular bond is not the whole picture, as it can lead to erroneous interpretations of the bond in diatomic molecules and fails to predict the dipole moment of diatomics. Thanks to machine learning, we can predict the dipole moment of any diatomic molecule in less than a second, whereas a typical CCSD(T) calculation would take hours. Similarly, we can uncover unexpected correlations between the dipole moment

https://doi.org/10.1021/acsomega.5c09766
ACS Omega 2026, 11, 17286−17291

and the atomic properties of its constituent atoms, helping us better understand the structure of the periodic table and the nature of the dipole moment.

In a more practical sense, and answering the question of the title of this paper, thanks to a fast screening of diatomic molecules via machine learning techniques, we conclude that the molecules with the largest dipole moment are heavy halogens combined with heavy alkali atoms and alkali-Au molecules, all of them showing dipole $\gtrsim$11 D. Furthermore, we provide an analytical expression for the dipole moment of diatomics derived via symbolic regression, which is the most accurate expression to date for predicting the dipole moment of any diatomic molecule. Our model only requires atomic properties accessible to any user. Finally, it is worth emphasizing that our machine learning model can predict the dipole moment of molecules containing a specific atom, thereby opening a new avenue for identifying the optimal molecule for testing physics beyond the standard model. However, the dipole moment cannot be solely the result of the atomic properties of a molecule's constituent atoms; it must depend on molecular properties, and therefore our approach is not more accurate.

■ ASSOCIATED CONTENT

Supporting Information

The Supporting Information is available free of charge at https://pubs.acs.org/doi/10.1021/acsomega.5c09766.

Details on the machine learning models; analysis on the relevance of features employed in the machine learning models; description of the quantum chemistry calculations of the dipole moment; and full data set on the dipole moment of diatomics, including references (PDF)

■ AUTHOR INFORMATION

Corresponding Author

Jesús Pérez-Ríos − *Department of Physics and Astronomy, Stony Brook University, Stony Brook, New York 11794, United States;* orcid.org/0000-0001-9491-9859; Email: jesus.perezrios@stonybrook.edu

Authors

Ahmed Elhalawani − *Department of Physics and Astronomy, Stony Brook University, Stony Brook, New York 11794, United States*

Ruiren Shi − *Department of Physics and Astronomy, Stony Brook University, Stony Brook, New York 11794, United States*

Mateo Londoño − *Department of Physics and Astronomy, Stony Brook University, Stony Brook, New York 11794, United States*

Michał Tomza − *Faculty of Physics, University of Warsaw, 02-093 Warsaw, Poland;* orcid.org/0000-0003-1792-8043

Complete contact information is available at: https://pubs.acs.org/10.1021/acsomega.5c09766

Notes

The authors declare no competing financial interest.

■ ACKNOWLEDGMENTS

The authors acknowledge the support of the United States Air Force Office of Scientific Research [Grant Number FA9550-23-1-0202]. M.T. acknowledges the National Science Centre Poland (Grant No. 2021/43/B/ST4/03326) for financial support.

■ ADDITIONAL NOTES

[1]The main difference is in HF since Pauling assumed a 63 % of partial ionic character, whereas Hannay and Smyth assumed a 41%.

[2]Note that in the original van Arkel−Ketelaar's triangle, compounds in the left corner are classified as metallic rather than van der Waals.

■ REFERENCES

(1) Rabideau, B. D.; Soltani, M.; Parker, R. A.; Siu, B.; Salter, E. A.; Wierzbicki, A.; West, K. N.; Davis, J. H. Tuning the melting point of selected ionic liquids through adjustment of the cation's dipole moment. *Phys. Chem. Chem. Phys.* **2020**, *22*, 12301−12311.

(2) Chernyak, Y. Dielectric Constant, Dipole Moment, and Solubility Parameters of Some Cyclic Acid Esters. *Journal of Chemical & Engineering Data* **2006**, *51*, 416−418.

(3) Mikaeeli, A.; Korte, D.; Rerek, T.; Chomicki, D.; Gündüz, B.; Derkowska-Zielinska, B.; Wieck, A. D.; Krupka, O.; Pawlak, M. Influence of the Dipole Moment on the Increase in the Thermal Conductivity of Thin Films Functionalized with Azo Dye. *J. Phys. Chem. C* **2024**, *128*, 15558−15565.

(4) Ni, K.-K.; Rosenband, T.; Grimes, D. D. Dipolar exchange quantum logic gate with polar molecules. *Chem. Sci.* **2018**, *9*, 6830−6838.

(5) Zhu, J.; Kais, S.; Wei, Q.; Herschbach, D.; Friedrich, B. Implementation of quantum logic gates using polar molecules in pendular states. *J. Chem. Phys.* **2013**, *138*, No. 024104.

(6) DeMille, D. Quantum Computation with Trapped Polar Molecules. *Phys. Rev. Lett.* **2002**, *88*, No. 067901.

(7) Bohn, J. L.; Rey, A. M.; Ye, J. Cold molecules: Progress in quantum engineering of chemistry and quantum matter. *Science* **2017**, *357*, 1002−1010.

(8) Schäfer, F.; Fukuhara, T.; Sugawa, S.; Takasu, Y.; Takahashi, Y. Tools for quantum simulation with ultracold atoms in optical lattices. *Nature Reviews Physics* **2020**, *2*, 411−425.

(9) Pérez-Ríos, J. *An Introduction to Cold and Ultracold Chemistry*; Springer International Publishing: Cham, Switzerland, 2020.

(10) Kruckenhauser, A.; Sieberer, L. M.; De Marco, L.; Li, J.-R.; Matsuda, K.; Tobias, W. G.; Valtolina, G.; Ye, J.; Rey, A. M.; Baranov, M. A.; Zoller, P. Quantum many-body physics with ultracold polar molecules: Nanostructured potential barriers and interactions. *Phys. Rev. A* **2020**, *102*, No. 023320.

(11) Micheli, A.; Brennen, G. K.; Zoller, P. A toolbox for lattice-spin models with polar molecules. *Nat. Phys.* **2006**, *2*, 341−347.

(12) Pérez-Ríos, J.; Herrera, F.; Krems, R. V. External field control of collective spin excitations in an optical lattice of $^2\Sigma$ molecules. *New J. Phys.* **2010**, *12*, 103007.

(13) Carr, L. D.; DeMille, D.; Krems, R. V.; Ye, J. Cold and ultracold molecules: science, technology and applications. *New J. Phys.* **2009**, *11*, No. 055049.

(14) Blackmore, J. A.; Caldwell, L.; Gregory, P. D.; Bridge, E. M.; Sawant, R.; Aldegunde, J.; Mur-Petit, J.; Jaksch, D.; Hutson, J. M.; Sauer, B. E.; Tarbutt, M. R.; Cornish, S. L. Ultracold molecules for quantum simulation: rotational coherences in CaF and RbCs. *Quantum Sciences and Techonology* **2019**, *4*, No. 014010.

(15) Smucker, J.; Pérez-Ríos, J. Alignment transport between ultracold polar molecules. *Phys. Chem. Chem. Phys.* **2024**, *26*, 21513−21519.

(16) Kłos, J.; Li, H.; Tiesinga, E.; Kotochigova, S. Prospects for assembling ultracold radioactive molecules from laser-cooled atoms. *New J. Phys.* **2022**, *24*, No. 025005.

(17) Marc, A.; Hubert, M.; Fleig, T. Candidate molecules for next-generation searches of hadronic charge-parity violation. *Phys. Rev. A* **2023**, *108*, No. 062815.
(18) Garcia Ruiz, R. F.; et al. Spectroscopy of short-lived radioactive molecules. *Nature* **2020**, *581*, 396−400.
(19) Udrescu, S. M.; et al. Isotope Shifts of Radium Monofluoride Molecules. *Phys. Rev. Lett.* **2021**, *127*, No. 033001.
(20) Zapata, J. C.; McKemmish, L. K. Computation of Dipole Moments: A Recommendation on the Choice of the Basis Set and the Level of Theory. *J. Phys. Chem. A* **2020**, *124*, 7538−7548.
(21) Ghosh, D. C.; Chakraborty, T. Computation of the dipole moments of some heteronuclear diatomic molecules in terms of the revised electronegativity scale of Gordy. *Journal of Molecular Structure: THEOCHEM* **2009**, *916*, 47−52.
(22) Pauling, L. The nature of the chemical bond. Application of results obtained from the quantum mechanics and from a theory of paramagnetic susceptibility to the structure of molecules. *J. Am. Chem. Soc.* **1931**, *53*, 1367−1400.
(23) Pauling, L. *The nature of the chemical bond and the structure of molecules and crystals: An introduction to modern structural chemistry*; Cornell University Press: Ithaca, N.Y., 1986.
(24) Hannay, N. B.; Smyth, C. P. The Dipole Moment of Hydrogen Fluoride and the Ionic Character of Bonds. *J. Am. Chem. Soc.* **1946**, *68*, 171−173.
(25) Klessinger, M. Polarity of Covalent Bonds. *Angewandte Chemie International Edition in English* **1970**, *9*, 500−512.
(26) Śmiałkowski, M.; Tomza, M. Highly polar molecules consisting of a copper or silver atom interacting with an alkali-metal or alkaline-earth-metal atom. *Phys. Rev. A* **2021**, *103*, No. 022802.
(27) Coulson, C. A. *Valence*; Clarendon Press, Oxford: Oxford, United Kingdom, 1952.
(28) Liu, L.-R.; Aguirre, M.; Kane, S. R.; Kendrick, B. K.; Hemmerling, B. Measurement of the electric dipole moment of AlCl by Stark-level spectroscopy. *Phys. Rev. A* **2025**, *111*, No. 062810.
(29) Zhang, R.; Steimle, T. C.; Cheng, L.; Stanton, J. F. The permanent electric dipole moment of gold chloride, AuCl. *Mol. Phys.* **2015**, *113*, 2073−2080.
(30) Wang, H.; Zhuang, X.; Steimle, T. C. The permanent electric dipole moments of cobalt monofluoride, CoF, and monohydride, CoH. *J. Chem. Phys.* **2009**, *131*, 114315.
(31) Zhuang, X.; Steimle, T. C. The electric dipole moment of cobalt monoxide, CoO. *J. Chem. Phys.* **2014**, *140*, 124301.
(32) Koelemay, L. A.; Ziurys, L. M. Elusive Iron: Detection of the FeC Radical ($X^3\Delta_i$) in the Envelope of IRC+10216. *Astrophysical Journal Letters* **2023**, *958*, L6.
(33) Steimle, T. C.; Chen, J.; Harrison, J. J.; Brown, J. M. A molecular-beam optical Stark study of lines in the (1,0) band of the $F^4\Delta_{7/2}$-$X^4\Delta_{7/2}$ transition of iron monohydride, FeH. *J. Chem. Phys.* **2006**, *124*, 184307.
(34) DeLeeuw, F. A.; Dymanus, A. Microwave spectrum and molecular parameters of cobalt monofluoride, CoF. *J. Mol. Spectrosc.* **1973**, *48*, 427−442.
(35) Le, A.; Steimle, T. C.; Skripnikov, L.; Titov, A. V. The molecular frame electric dipole moment and hyperfine interactions in hafnium fluoride, HfF. *J. Chem. Phys.* **2013**, *138*, 124313.
(36) Zhuang, X.; Steimle, T. C.; Linton, C. The electric dipole moment of iridium monofluoride, IrF. *J. Chem. Phys.* **2010**, *133*, 164310.
(37) Wang, H.; Virgo, W. L.; Chen, J.; Steimle, T. C. Permanent electric dipole moment of molybdenum carbide. *J. Chem. Phys.* **2007**, *127*, 124302.
(38) Fletcher, D. A.; Dai, D.; Steimle, T. C.; Balasubramanian, K. The permanent electric dipole moment of NbN. *J. Chem. Phys.* **1993**, *99*, 9324−9325.
(39) Qin, C.; Zhang, R.; Wang, F.; Steimle, T. C. The permanent electric dipole moment and hyperfine interactions in platinum monofluoride, PtF. *J. Chem. Phys.* **2012**, *137*, No. 054309.
(40) Steimle, T. C.; Jung, K. Y.; Li, B. The permanent electric dipole moment of PtO, PtS, PtN, and PtC. *J. Chem. Phys.* **1995**, *103*, 1767−1772.
(41) Steimle, T. C.; Virgo, W. L. The permanent electric dipole moments of WN and ReN and nuclear quadrupole interaction in ReN. *J. Chem. Phys.* **2004**, *121*, 12411−12420.
(42) Gengler, J.; Ma, T.; Adam, A. G.; Steimle, T. C. A molecular beam optical Stark study of the [15.8] and [16.0] $2\Pi_{1/2}$-$X^4\Sigma^-$ (0,0) band systems of rhodium monoxide, RhO. *J. Chem. Phys.* **2007**, *126*, 134304.
(43) Steimle, T. C.; Virgo, W. L.; Ma, T. The permanent electric dipole moment and hyperfine interaction in ruthenium monoflouride (RuF). *J. Chem. Phys.* **2006**, *124*, No. 024309.
(44) Wang, F.; Steimle, T. C. Communication: Electric dipole moment and hyperfine interaction of tungsten monocarbide, WC. *J. Chem. Phys.* **2011**, *134*, 201106.
(45) Ladjimi, H.; Tomza, M. Diatomic molecules of alkali-metal and alkaline-earth-metal atoms: Interaction potentials, dipole moments, and polarizabilities. *Phys. Rev. A* **2024**, *109*, No. 052814.
(46) Tomza, M. Prospects for ultracold polar and magnetic chromium−closed-shell-atom molecules. *Phys. Rev. A* **2013**, *88*, No. 012519.
(47) Tomza, M. Interaction potentials, electric moments, polarizabilities, and chemical reactions of YbCu, YbAg, and YbAu molecules. *New J. Phys.* **2021**, *23*, No. 085003.
(48) Liu, X.; McKemmish, L.; Pérez-Ríos, J. The performance of CCSD(T) for the calculation of dipole moments in diatomics. *Phys. Chem. Chem. Phys.* **2023**, *25*, 4093−4104.
(49) Allen, L. C.; Capitani, J. F.; Kolks, G. A.; Sproul, G. D. Van Arkel—Ketelaar triangles. *J. Mol. Struct.* **1993**, *300*, 647−655.
(50) Ketelaar, J. A. A. *Chemical Constitution: An Introduction to the Theory of the Chemical Bond*; Elsevier Publishing Company: Houston, 1953; p 398.
(51) Williams, C. K.; Rasmussen, C. E. *Gaussian processes for machine learning*; MIT Press: Cambridge, MA, 2006; vol 2.
(52) Liu, X.; Meijer, G.; Pérez-Ríos, J. On the relationship between spectroscopic constants of diatomic molecules: a machine learning approach. *RSC Adv.* **2021**, *11*, 14552−14561.
(53) Liu, X.; Meijer, G.; Pérez-Ríos, J. A data-driven approach to determine dipole moments of diatomic molecules. *Phys. Chem. Chem. Phys.* **2020**, *22*, 24191−24200.
(54) Hou, S.; Bernath, P. F. Relationships between dipole moments of diatomic molecules. *Phys. Chem. Chem. Phys.* **2015**, *17*, 4708−4713.
(55) Hou, S.; Bernath, P. F. Relationship between Dipole Moments and Harmonic Vibrational Frequencies in Diatomic Molecules. *J. Phys. Chem. A* **2015**, *119*, 1435−1438.
(56) Pereira, F.; Aires-de Sousa, J. Machine learning for the prediction of molecular dipole moments obtained by density functional theory. *J. Cheminf.* **2018**, *10*, 43.
(57) Veit, M.; Wilkins, D. M.; Yang, Y.; DiStasio, J.; Robert, A.; Ceriotti, M. Predicting molecular dipole moments by combining atomic partial charges and atomic dipoles. *J. Chem. Phys.* **2020**, *153*, No. 024113.
(58) Wayo, D. D. K.; Noor, M. Z. B. M.; Ganji, M. D.; Saporetti, C. M.; Goliatt, L. Q-DFTNet: A Chemistry-Informed Neural Network Framework for Predicting Molecular Dipole Moments via DFT-Driven QM9 Data. *J. Comput. Chem.* **2025**, *46*, No. e70206.
(59) Cranmer, M. Interpretable Machine Learning for Science with PySR and SymbolicRegression.jl. 2023; http://arxiv.org/abs/2305.01582, arXiv:2305.01582 [astro-ph, physics:physics].

https://doi.org/10.1021/acsomega.5c09766
ACS Omega 2026, 11, 17286−17291